International Journal of Mechanical and Production Engineering Research and Development (IJMPERD)
ISSN(P): 2249-6890; ISSN(E): 2249-8001
Vol. 3, Issue 5, Dec 2013, 49-56

BREAKUP OF LIQUID SHEET ANALYSIS WHEN PRESSED BETWEEN TWO GAS STREAMS

MAYUR R. MOGRE

[1]Undergraduate Student, Jawaharlal Darda Institute of Engineering and Technology, Yavatmal, Maharashtra, India

ABSTRACT

Formation of droplets due to breakup of liquid column is important research. In the present study break up of planer liquid sheet has been investigated using linear stability analysis.In this study both sinuous and varicose modes of disturbance are used. As reported by the earlier studies linear analysis of sinuous mode will not create any breakup of the liquid sheet but linear analysis of varicose mode of disturbance can create breakup of the liquid sheet. Also breakup of the liquid sheet is very much nonlinear especially at the time of break up. So a nonlinear analysis is required for the complete understanding of the underlying physics of the breakup process. But which will be the dominant mode of break up process and what will be the frequency and growth rate of fundamental mode of perturbation can be assessed by the linear analysis. So in this study temporal linear stability analysis has been done for both sinuous and varicose modes of disturbance to calculate the growth rate and frequency. The result shows very good agreement with the earlier studies. Parametric studies to understand the influence of fluid velocity ratio, density ratio and surface tension on the growth rate have also been investigated.

KEYWORDS: Planar Liquid Sheet, Temporal Stability, Linear Stability Analysis

Nomenclature

Table 1

h	Half thickness of liquid sheet (m)
k	Wave number (dimensionless)
k_c	Cut-off wave number (dimensionless)
k_{max}	Critical wave number, corresponding to maximum growth rate (dimensionless)
L	Non-dimensional break-up length
l	Break-up length of the liquid sheet
U	Gas-to-liquid velocity ratio, u_g/u_l
u_l	Velocity of the liquid sheet
u_g	Velocity of the gaseous phase
We	Weber number (= $\rho_l u_l^2 h / \sigma$) (dimensionless)
x	Axial coordinate (m)
y	Transverse coordinate (m)
Greek Symbols	
α	Angular frequency (dimensionless)
β	Growth rate (dimensionless)
β_{max}	Maximum growth rate (dimensionless)
ϕ	Dimensionless velocity potential
$\eta(x,t)$	Instantaneous and local transverse coordinate of interface (dimensionless)
η_0	Initial disturbance amplitude (dimensionless)
ψ	Function representing temporal variation of η
ω	Temporal frequency
ρ_l	Liquid density

Table 1 Contd.,

ρ	Gas-to-liquid density ratio
ρ_g	Gas density (kg/m^3)
σ	Surface tension coefficient
μ_g	Viscosity of gas
μ_l	Viscosity of liquid
Subscripts	
g	Gas phase
1	Top interface (j = 1 or 2)
2	Bottom interface
l	Liquid phase
n	nth order
$,t$	$\partial / \partial t$
$,x$	$\partial / \partial x$
$,xx$	$\partial^2 / \partial x^2$
$,xy$	$\partial^2 / \partial x \partial y$
$,y$	$\partial / \partial y$
$,yy$	$\partial^2 / \partial y^2$

INTRODUCTION

Liquid sprays are encountered in nature and in a wide range of science and engineering applications. It generally consists of different sizes of droplets dispersed in a gaseous medium. In nature, droplets can be found as rain, dew, fog, clouds and waterfall mist. Mechanical devices like nozzles or atomizers also produce spray. In many industrial applications liquid is used as a spray instead of bulk liquid such as spray drying, spray cooling, spray combustion, spray deposition, thermal spray, surface treatment, spray inhalation, crop spray, spray painting etc. So spray has become a subject of interest in many engineering disciplines like mechanical, aerospace, chemical, metallurgy, materials, pharmaceutical, food processing, and agriculture, meteorology and powder generation. Atomization of the bulk liquid can be achieved in different ways, such as aerodynamically, mechanically, ultrasonically, or electro statically. Depending upon the atomization process droplet size in the spray will also vary. In most of the atomizers, droplet size generally varies from a few microns to around 800 - 1000 microns.

For sprays in agriculture and fire suppression system, the droplets should be sufficiently large to have enough momentum so that they could not be carried away by the wind. On the other hand, bronchial sprays require very small droplets of the order of few microns, so that the droplets can pass through the small airways and reach the lung. Therefore disintegration of liquid sheets and leading to generation of fine droplets has been extensively investigated owing to its importance in atomization and spray formation. Excellent reviews on the subject are available in Lin and Reitz [1], Mehring and Sirignano [2] and Lin [3]. The injector configuration can be idealized as a liquid sheet sandwiched between two gas streams. Annular liquid sheets, which are the configuration of the liquid sheet emerging from most of the atomizers, can also be reasonably simplified to a planar liquid sheet sandwiched between two planar gaseous layers if the sheet thickness is much smaller than the mean radius of the annulus.

Earlier studies reported that, though the fundamental sinuous mode generally grows at a much faster rate than the varicose mode over a wide range of parameters, still this mode alone cannot cause breakup as the distance between the two surfaces are preserved for linear stability analysis. It is the varicose mode, which in spite of low growth rate, causes the instability by bringing the surfaces closer. Mitra et al. [4] Nath et al [5] investigated the linear stability of a planar liquid

sheet subjected to both sinuous and varicose disturbance. The sinuous mode was observed to be responsible for large amplitude deformation while the varicose mode caused the breakup.

The objective of the present work is to investigate the effect of velocity ratio, density ratio and surface tension on growth rate of disturbance for both the sinuous and varicose mode of disturbance.

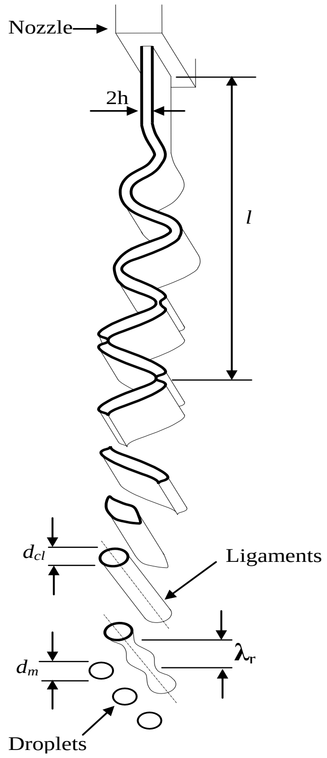

Figure 1: Schematic Diagram of a Planer Sheet Breakup Leading to Spray Formation Ref [7]

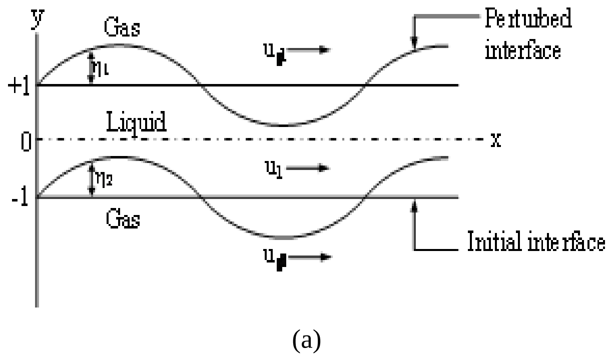

(a)

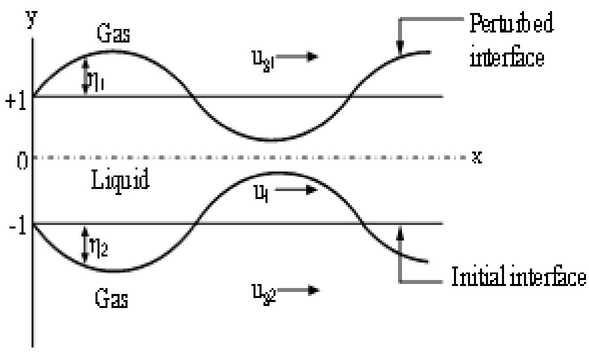

(b)

Figure 2: Schematic of the Liquid Sheet Interface for (a) Sinuous (b) Varicose Mode of Disturbances

MATHEMATICAL FORMULATIONS

Figures 2(a) and 2(b) shows the schematic of a planner liquid sheet surrounding with two gas streams moving with non zero velocities and the gas-liquid interfaces for sinuous and varicose mode of disturbances respectively. In the undisturbed state, one-dimensional flow is assumed and the velocity of the liquid sheet is given by u_l while that of each gas medium is given by u_g. The densities of gas and liquid layers are given by ρ_g and ρ_l respectively. Froude number for typical atomizer conditions are generally being high, the effect of gravity has been neglected for the analysis. Cousin and Domouchel [6] have shown that for high Weber number $(We_g^2 / \mathrm{Re}_l < 10^{-3})$ the effect of viscosity on the stability of a planar liquid sheet can also be neglected.

For the convenience of analysis, all the physical parameters are non-dimensionalized. Length is non-dimensionalized by half-sheet thickness h, time by the onvection time h/ul where ul is the velocity of the undisturbed liquid sheet, and density by liquid density ρl

When the undisturbed flow, described above, is perturbed by a small disturbance, the positions of the two interfaces are described as

$$y(x,t) = (-1)^{j+1} + \eta_j(x,t) \tag{1}$$

In the above equation, j = 1 and 2 denote the upper and the lower interface respectively. The resulting velocity field must satisfy the equation for conservation of mass. The interfaces must satisfy the kinematic and the dynamic boundary conditions. The surface deformations $\eta_j(x,t)$ must satisfy the above governing equations and boundary conditions. The solution to the above is obtained using regular perturbation theory with the initial (small) disturbance amplitude η_0 as the perturbation parameter. The surface deformation is expanded in a power series of η_0 as

$$\eta_j(x,t) = \sum_{n=1}^{\infty} \eta_0^n \eta_{jn}(x,t) \tag{2}$$

Following the analysis of Ibrahim and Jog [9] and Nath et al. [5], the present study will focus on the first order solutions only. The governing equations and the boundary conditions for the first order linear stability analysis are as follows.

Governing Equations

$$\phi_{l1,xx} + \phi_{l1,yy} = 0\,,\ -1+\eta_2 \le y \le 1+\eta_1 \tag{3}$$

$$\phi_{gj1,xx} + \phi_{gj1,yy} = 0\ ;$$

$$-H \le y \le 1+\eta_2, -1+\eta_1 \le y \le H \tag{4}$$

Kinematic Boundary Conditions

$$\phi_{l1,y} - \eta_{j1,t} - \eta_{j1,x} = 0 \tag{5}$$

$$\phi_{gj1,y} - \eta_{j1,t} - U\eta_{j1,x} = 0 \tag{6}$$

Dynamic Boundary Conditions

$$\rho\phi_{gj1,t} - \phi_{l1,t} + \rho U\phi_{gj,x} - \phi_{l1,x} = \frac{(-1)^j}{We}\eta_{j,xx} \tag{7}$$

Solution Procedure

Solution for Sinuous Mode

Two major modes of disturbance are generally considered in stability analysis of liquid sheet. Sinuous (when the disturbances on the two surfaces of the liquid sheet are in phase) and varicose (when the disturbances on the two surfaces have a phase difference of 180°). The two modes of disturbance are shown schematically in Figure 2.

If the initial amplitude of disturbance is η_0 and wave number is k, then the profile of the perturbed surface can be described in linear stability analysis by the function

$$\eta_j(x,t) = \eta_0\left[\psi_{j1}(t)\exp(ikx) + \bar{\psi}_{j1}(t)\exp(-ikx)\right] \tag{8}$$

Here, $\bar{\psi}_{j1}(t)$ denotes the complex conjugate of $\psi_{j1}(t)$.

Substitution of Eq. (8) in the kinematic boundary conditions, Eqs. (5) and (6) and using the governing equations, Eqs. (3) and (4), the velocity potentials for the upper gas, lower gas and liquid sheet are obtained. Substituting the expressions of the velocity potentials and the surface deformation in the dynamic boundary condition, Eq.(7), the following dispersion equation is obtained:

$$\begin{aligned}&\frac{1}{k}\left[\tanh(k)+\rho\right]\psi_{j1,tt} + 2i\left[\tanh(k)+\rho U\right]\psi_{j1,t}\\ &-\left[k\tanh(k)+\rho kU^2 - \frac{k^2}{We}\right]\psi_{j1} = 0\end{aligned} \tag{9}$$

The solution of Eq. (9) gives the functional form of $\psi_{j1}(t)$.

It may be noted that for temporal stability analysis, the wave number k is real while the temporal frequency, ω_1 is complex, given by $\omega_1 = \alpha_1 + i\beta_1$, where α_1 and β_1 represent the angular frequency and the growth rate respectively. The initial conditions used to obtain the solution are as follows.

$$\begin{aligned}&\eta_{j1}(x,0) = \cos(kx)\\ &\eta_{j1,t}(x,0) = -\alpha_1\sin(kx)\end{aligned} \tag{10}$$

Applying the above initial conditions, the following solution is obtained:

$$\psi_{j1}(t) = \frac{1}{2}\cosh(\beta_1 t)\exp(i\alpha_1 t) \tag{11}$$

The growth rate and the angular frequency are given by

$$\beta_1 = \frac{k\left\{\rho(1-U)^2\tanh(k) - \frac{k}{We}\left(\rho+\tanh(k)\right)\right\}^{1/2}}{\rho+\tanh(k)} \tag{12}$$

and $\alpha_1 = -\dfrac{k\left(\rho U + \tanh(k)\right)}{\rho + \tanh(k)}$ (13)

respectively.

Solution for Varicose Mode

The analysis for the varicose mode is similar to that of the sinuous mode. However, as shown in Figure 2(b), the deformation of the liquid sheet is symmetric about the mid-plane of the liquid sheet. Thus, only one half of the domain needs to be computed using symmetry condition at the central axis (y = 0). The symmetry conditions require that the normal velocity and the normal gradient of the axial velocity are zero. In terms of the velocity potential of the liquid, these conditions become

$$\phi_{l,y} = \phi_{l,xy} = 0 \tag{14}$$

Proceeding similarly as in the case of sinuous mode, the first order dispersion relation, growth rate and angular frequency are obtained as

$$\begin{aligned} &\frac{1}{k}\left[\coth(k) - \rho\right]\psi_{j1,tt} + 2i\left[\coth(k) + \rho U\right]\psi_{j1,t} \\ &-k\left[\coth(k) + \rho U^2 - \frac{k}{We}\right]\psi_{j1} = 0 \end{aligned} \tag{15}$$

$$\beta_1 = \frac{k\left\{\rho(1-U)^2\coth(k) - \dfrac{k}{We}\left(\rho + \coth(k)\right)\right\}^{1/2}}{\rho + \coth(k)} \tag{16}$$

$$\alpha_1 = -\frac{k\left(\rho U + \coth(k)\right)}{\rho + \coth(k)} \tag{17}$$

Fractional powers are preferred to root signs. The solidus (/) should be used instead of the horizontal line for fractions whenever possible. Consecutive numbers to identity mathematical expressions should be enclosed in parentheses. Refer to equations in the text as "Eq.(1),"etc., or "Equation(1)," etc., at the beginning of a sentence. All symbols should be in italic letters.**4.**

RESULTS AND DISCUSSIONS

At all wave numbers and for U < 1, the growth rate for the sinuous mode is at least one order of magnitude higher than that for the varicose mode. From Figure 3 it is also clear that for the stability curves for U > 1 and U < 1 the cut-off frequency does not depend as strongly on the velocity ratio for U < 1 as in the case of U > 1. Figure 3 also shows the variation of maximum growth rate, $\beta_{\max}$ with velocity ratio for both sinuous and varicose modes at different Weber numbers. The figure shows that for U < 1, $\beta_{\max}$ remain invariant with U except for the region close to U ~ 1.

For values of U close to 1, the growth rate sharply decreases for both sinuous and varicose modes. In this formulation, the instability is primarily driven by the velocity difference across the interface. Hence, for velocity ratios close to 1, this driving factor gets weakened, leading to small growth rates. From the figure, it is also observed that for all Weber numbers and U < 1, the growth rate is higher for sinuous mode.

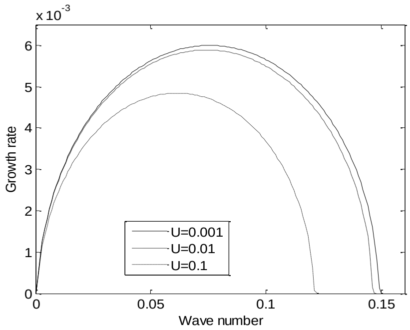

(a) We=150 rho=.001 and U<1, Sinuous Mode of Disturbance

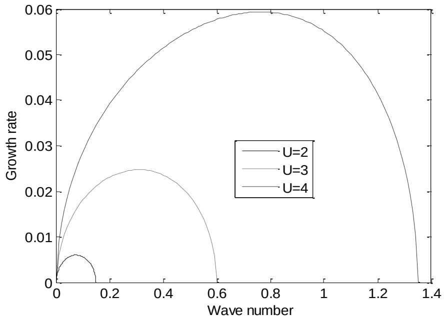

(b) We=150 rho=.001 and U>1, Sinuous Mode of Disturbance

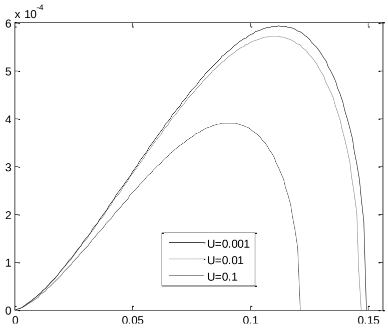

(c) We=150 rho=.001 and U<1, Varicose Mode of Disturbance

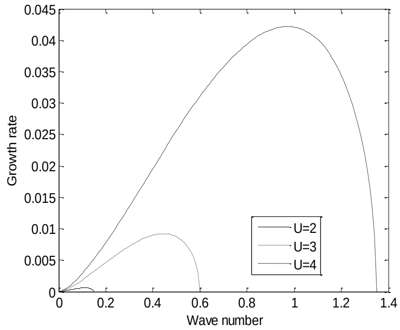

(d) We=150 rho=.001 and U>1, Varicose Mode of Disturbance

Figure 3: Variation of Growth Rate with Wave Number for Different Velocity Ratio

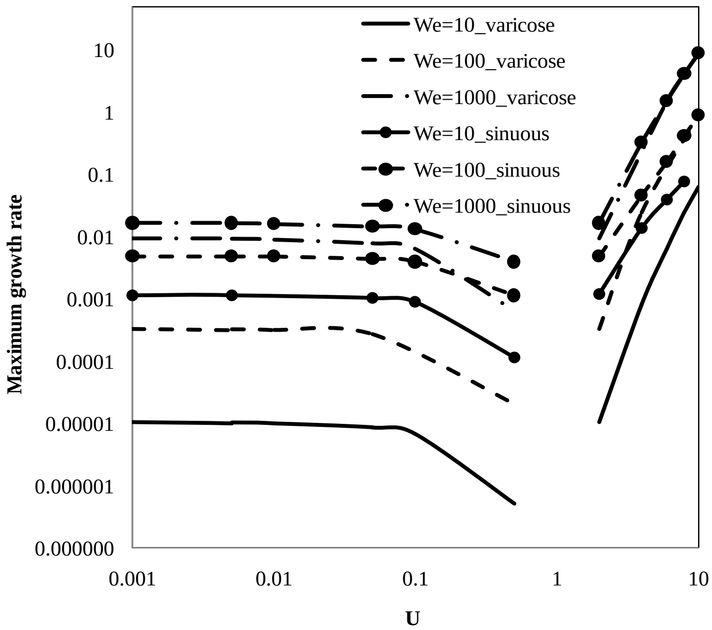

Figure 4: Variation of Maximum Growth Rate with Velocity Ratio for Different Weber Numbers

For U > 1, both these parameters increase with velocity ratio and at very high velocity ratios, the sinuous and the varicose modes have similar maximum growth rate. The range of velocity ratios for which the two modes show similar instability characteristics increases with increasing Weber number. Figure 4 shows the variation maximum growth rate with velocity ratio for different Weber number. The growth rate is higher for sinuous mode than for varicose mode, but the difference decreases with increase in Weber number.

CONCLUSIONS

A linear model has been developed for predicting the growth rate of breakup for a planar liquid sheet sandwiched between two moving gas streams. The velocity of the gas streams is taken to be equal but different from that of the liquid sheet. Closed form solutions for the gas and liquid velocity fields and the interface shape are obtained assuming inviscid, irrotational flow for both the phases. The effects of gas velocity, both higher and lower than the liquid velocity, are investigated for a wide range of Weber number .The major observations of the investigation is for $U < 1$, the growth rate is higher for sinuous mode at all Weber numbers. However, for $U > 1$, the growth rates for sinuous and varicose modes become similar at high velocity ratios.

REFERENCES

1. Lin, S.P. and Reitz, R.Z., “Drop and spray formation from a liquid jet, Annual Reviews in Fluid Mechanics,” vol. 30, 1998, pp. 85 – 105.

2. Sirignano, W.A. and Mehring, C., “Review of theory of distortion and disintegration of liquid streams,” Progress in Energy and Combustion Science, vol. 26, 2000, pp. 609 – 655.

3. Lin, S.P., “Breakup of Liquid Sheets and Jets,” Cambridge University Press, Cambridge,2003.

4. Mitra, S.K., Li, X. and Renksizbulut, M., “On the breakup of liquid sheets by dual-mode linear analysis,” AIAA Journal of Propulsion and Power, vol. 17,2001, pp. 728 – 735.

5. Nath, S., Mukhopadhyay, A., Datta, A., Sen, S. and Tharakan, T. J., “Influence of gas velocity on breakup of planar liquid sheets sandwiched between two gas streams,” Atomization and Sprays, vol.20(11),2010, pp.983-1003.

6. Cousin, J., Yoon, S.J. and Dumouchel, C., “Coupling of classical linear theory and maximum entropy formalism for prediction of drop-size distribution in sprays: application to pressure swirl atomizers.” Atomization Sprays, vol.6,1996, pp.601-622.

7. Nath, S., Mukhopadhyay, A., Datta, A., Sen, S. and Tharakan, T. J., “Prediction of size and velocity distributions in sprays formed by the breakup of planar liquid sheets using maximum entropy formalism,”*Atomization and Sprays*, 21 (6),2011, 483–501.

8. Squire, H. B., “Investigation of the Instability of a Moving Liquid Film,” British Journal of Applied Physics, vol.4,1953, pp.167-169.

9. Ibrahim, A.A. and Jog, M.A., “Nonlinear instability of an annular liquid sheet exposed to gas flow,” International Journal of Multiphase Flow, vol.34, 2008, pp.647 – 664.